

Weak lensing in the second post-Newtonian approximation: Gravitomagnetic potentials and the integrated Sachs-Wolfe effect

B. M. Schäfer^{1*} and M. Bartelmann^{2*}

¹Max-Planck-Institut für Astrophysik, Karl-Schwarzschild-Straße 1, Postfach 1317, 85741 Garching, Germany

²Institut für theoretische Astrophysik, Universität Heidelberg, Albert-Ueberle-Straße 2, 69120 Heidelberg, Germany

6 December 2018

ABSTRACT

Dark matter currents in the large-scale structure give rise to gravitomagnetic terms in the metric, which affect the light propagation. Corrections to the weak lensing power spectrum due to these gravitomagnetic potentials are evaluated by perturbation theory. A connection between gravitomagnetic lensing and the integrated Sachs-Wolfe (iSW) effect is drawn, which can be described by a line-of-sight integration over the divergence of the gravitomagnetic vector potential. This allows the power spectrum of the iSW-effect to be derived within the framework of the same formalism as derived for gravitomagnetic lensing and reduces the iSW-effect to a second order lensing phenomenon. The three-dimensional power spectra are projected by means of a generalised Limber-equation to yield the angular power spectra. While gravitomagnetic corrections to the weak lensing spectrum are negligible at observationally accessible scales, the angular power spectrum of the iSW-effect should be detectable as a correction to the CMB spectrum up to multipoles of $\ell \approx 100$ with the *Planck*-satellite.

Key words: gravitational lensing, cosmology: large-scale structure, cosmic microwave background, methods: analytical

1 INTRODUCTION

Cosmological weak lensing (Bartelmann & Schneider 2001) has evolved to be a valuable tool in cosmology. Weak lensing surveys have contributed significantly to the determination of the dark matter power spectrum and to the estimation of its amplitude σ_8 (Schneider et al. 1998; van Waerbeke et al. 2000) by the measurement of cosmic shear and have enabled the reconstruction of the dark matter distribution in rich clusters of galaxies (e.g. Kaiser & Squires 1993; Seitz et al. 1996; Ménard et al. 2003).

So far, only static matter distributions have been considered but from the solution to Maxwell’s equations in the framework of general relativity it follows that gravitomagnetic potentials generated by moving masses should alter the predictions for light deflection (Schneider et al. 1992). While gravitomagnetic corrections to lensing are small, being of order v/c , where v is the velocity of the deflecting mass, they may contribute to the weak cosmological lensing: The cluster peculiar velocities following from a cosmological N -body simulation like the Hubble-volume simulation (Colberg et al. 2000; Jenkins et al. 2001) are well described by a Gaussian distribution with zero mean and a standard deviation of $\sigma_v \approx 300$ km/s, which is a fraction of 10^{-3} of the speed of light. Thus, relativistic effects influence the lensing signal appreciably in $\lesssim 1\%$ of all clusters. In filaments (Colberg et al. 2004) where mat-

ter is funneled towards the clusters, velocities are even higher: Infall velocities up to a few 10^3 km/s have been measured.

The integrated Sachs-Wolfe (iSW) effect, or Rees-Sciama (RS) effect (Sachs & Wolfe 1967; Rees & Sciama 1968) arises if CMB photons encounter time-varying gravitational potentials on their passage from the last-scattering surface to the observer. When transversing time-varying potentials, the energy gains and losses a CMB photon experiences in entering and leaving potential wells do not cancel exactly. In this way, one expects a net blueshift of CMB photons in forming voids and a net redshift in matter-accreting clusters of galaxies.

The iSW/RS effect has been studied theoretically in individual objects (Martínez-González et al. 1990) and can be used for the investigation of cluster mergers (Rubiño-Martín et al. 2004). More importantly, it is sensitive to mapping the large-scale structure as it highlights the sites of active structure formation (Kaiser 1982; Martínez-González & Sanz 1990; Martínez-González et al. 1992, 1994; Seljak 1996). Furthermore, the iSW-effect may turn out to be a powerful probe for dark energy’s influence on structure formation (Crittenden & Turok 1996), when combined with other tracers of structure. A numerical approach has been undertaken by Tuluie & Laguna (1995a,b), who followed photons through a cosmological n -body simulation and carried out the line-of-sight integration numerically.

The aim of this paper is to determine the corrections to the power spectra of weak lensing quantities caused by gravitomagnetic terms and to derive the iSW power spectrum, both by apply-

* e-mail: spirou@mpa-garching.mpg.de (BMS); mbartelmann@ita.uni-heidelberg.de (MB)

ing perturbation theory. In comparison to preceding treatments by Seljak (1996) and Cooray (2002), the novel approach taken to determine the iSW power spectrum is by relating it to the gravitomagnetic terms in considered in lensing. Gravitomagnetic corrections to lensing have indeed been observed by Fomalont & Kopeikin (2003) in imaging radio waves from a quasar on Jupiter, which is an outstanding achievement in VLBI astrometry. Gravitomagnetic corrections to lensing in the large-scale structure would only be detectable by their n -point statistics or by topological measures like Minkowski functionals, that would be especially sensitive to the effect's intrinsic non-Gaussianity. Concerning the iSW-effect, there are a quite a few reports on its detection in WMAP data in cross correlation with various populations of tracer objects (Afshordi et al. 2004; Fosalba et al. 2003; Bouhgn & Crittenden 2004; Nolta et al. 2004; Hirata et al. 2004), but so far it has not been possible to derive values for single multipoles based on CMB data alone.

The paper is structured as follows: After a compilation of key formulae and the derivation of Limber's equation for vector fields in Sect. 2, the power spectrum of weak gravitational lensing is considered and the correction terms due to gravitomagnetic potentials are worked out by perturbation theory in Sect. 3. Then, the iSW-effect is related to gravitomagnetic lensing and its power spectrum is subsequently derived in a perturbative approach in Sect. 4. The results are summarised in Sect. 5.

2 KEY FORMULAE

The assumed cosmological model is the standard Λ CDM cosmology, which has recently been supported by observations of the WMAP satellite¹ (Spergel et al. 2003). Parameter values have been chosen as $\Omega_M = 0.3$, $\Omega_\Lambda = 0.7$, $H_0 = 100 h \text{ km s}^{-1} \text{ Mpc}^{-1}$ with $h = 0.7$, $\Omega_B = 0.04$, $n_s = 1$ and $\sigma_8 = 0.9$.

2.1 Structure formation

The cosmic density field ρ given in terms of the dimensionless density perturbation $\delta = (\rho - \langle \rho \rangle) / \langle \rho \rangle$, where $\langle \rho \rangle$ is the average density of matter. The 2-point correlation properties of the overdensity field δ are described by the power spectrum $P(k)$:

$$\langle \delta(\mathbf{k}) \delta^*(\mathbf{k}') \rangle = (2\pi)^3 \delta_D(\mathbf{k} - \mathbf{k}') P(k), \text{ where} \quad (1)$$

$$\delta(\mathbf{k}) = \int d^3x \delta(\mathbf{x}) \exp(i\mathbf{k}\mathbf{x}) \quad (2)$$

is the Fourier transform of the overdensity field δ . The normalisation of the power spectrum $P(k)$ is given by the parameter σ_8 , i.e. the variance of δ on scales of $R = 8 \text{ Mpc}/h$:

$$\sigma_R^2 = \frac{1}{2\pi^2} \int_0^\infty dk k^2 W^2(kR) P(k). \quad (3)$$

Here, W is a window function of top-hat shape, the Fourier-transform of which is given by:

$$W(x) = \frac{3}{x^3} [\sin(x) - x \cos(x)] = \frac{3}{x} J_1(x). \quad (4)$$

The shape of the power spectrum $P(k) \propto k^{n_s} \cdot T^2(k)$ is well approximated by the transfer functions $T(k)$ suggested by Bardeen et al. (1986). They read in case of adiabatic initial conditions:

$$T(q) = \frac{\ln(1 + 2.34q)}{2.34q} \left[1 + 3.89q + (16.1q)^2 + (5.46q)^3 + (6.71q)^4 \right]^{-\frac{1}{4}} \quad (5)$$

The wave vector k is commonly divided by the shape parameter Γ introduced by Efstathiou et al. (1992) for CDM models and extended to models with $\Omega \neq 1$ by Sugiyama (1995):

$$q = q(k) = \frac{k/\text{Mpc}^{-1}h}{\Gamma} \text{ with } \Gamma = \Omega_M h \exp \left(-\Omega_B \cdot \left[1 + \frac{\sqrt{2h}}{\Omega_M} \right] \right). \quad (6)$$

In linear structure formation, each Fourier-mode grows independently and at the same rate. The time dependence of the overdensity field δ can be described by the growth function $D(a)$:

$$\delta(a) = \delta_0 D(a) \text{ with } D(a) = a \frac{d'(a)}{d'(1)}. \quad (7)$$

The shape of $d'(a)$ is well approximated by the formula suggested by Carroll et al. (1992):

$$d'(a) = \frac{5}{2} \Omega_M(a) \left[\Omega_M^{4/7}(a) - \Omega_\Lambda(a) + \left(1 + \frac{\Omega_M(a)}{2} \right) \left(1 + \frac{\Omega_\Lambda(a)}{70} \right) \right]^{-1}. \quad (8)$$

2.2 Dark matter currents

The continuity equation $\dot{\rho} = -\text{div}(\rho\mathbf{v})$ requires the existence of large-scale coherent matter streams $\mathbf{j} = \rho\mathbf{v}$ superimposed on the Hubble flow due to the formation of structure. In Fourier space, the relation between density and velocity reads in the Eulerian frame in linear approximation:

$$\mathbf{v}(\mathbf{k}) = -iaH(a)f(\Omega) \frac{\mathbf{k}}{k^2} \delta(\mathbf{k}) = -i\dot{a}f(\Omega) \frac{\mathbf{k}}{k^2} \delta(\mathbf{k}). \quad (9)$$

The $1/k$ -dependence causes cosmological velocities to come predominantly from perturbations on larger scales in comparison to those that dominate the density field. $H(a) = d \ln(a)/dt$ is Hubble's function. The function f describes the dependence of the equation of continuity on cosmic time and is a function of the mass density Ω (Peebles 1980; Lahav et al. 1991):

$$f(\Omega) = \frac{d \ln \delta}{d \ln a} = \frac{d \ln D(a)}{d \ln a} \simeq \Omega(a)^{0.6} \quad (10)$$

In analogy to eqn. (7), time evolution of of dark matter current velocities in the comoving frame is described by $G(a)$,

$$G(a) = \frac{g'(a)}{g'(1)} \text{ with } g'(a) \equiv H(a)f(\Omega). \quad (11)$$

The theory of peculiar velocity fields is reviewed in detail in Dekel (1994) and Strauss & Willick (1995).

In general, the effects considered here are sensitive to density weighted velocities. The Fourier transform of vector fields $\mathbf{q}(\mathbf{x}) = \delta(\mathbf{x})\mathbf{v}(\mathbf{x})$ can be derived with the convolution theorem:

$$\mathbf{q}(\mathbf{k}) = \int d^3x \mathbf{q}(\mathbf{x}) \exp(i\mathbf{k}\mathbf{x}) \quad (12)$$

$$= \frac{1}{2} \int \frac{d^3p}{(2\pi)^3} [\mathbf{v}(\mathbf{p})\delta(\mathbf{k} - \mathbf{p}) + \mathbf{v}(\mathbf{k} - \mathbf{p})\delta(\mathbf{p})], \quad (13)$$

where the integrand has been symmetrised in eqn. (13).

2.3 Limber's equation for vector fields

For the derivation of the angular power spectrum of the gravitomagnetic corrections to weak cosmological lensing or that of the iSW-effect, a variant of Limber's equation is necessary that is able to deal with projections of vector fields $\mathbf{q}(\mathbf{x})$ instead of scalar fields.

¹ <http://map.gsfc.nasa.gov/>

The derivation presented here is generalised from Vishniac (1987). Consider a vector field $\mathbf{q}(\mathbf{x})$ and its Fourier transform $\mathbf{q}(\mathbf{k})$:

$$\mathbf{q}(\mathbf{x}) = \int \frac{d^3k}{(2\pi)^3} \mathbf{q}(\mathbf{k}) \exp(-i\mathbf{k}\mathbf{x}) \quad (14)$$

Any effect κ in question is assumed to measure a projection of $\mathbf{q}(\mathbf{x})$ on the line-of-sight, where \mathbf{e} is a unit tangent vector on the photon geodesic. $W(w)$ is a general weighing function dependent on the comoving distance w which describes its redshift dependence and is later to be replaced by e.g. the lensing efficiency function:

$$\kappa = \int_0^{w_{\max}} dw W(w) [\mathbf{e} \cdot \mathbf{q}] = \int_0^{w_{\max}} dw W(w) [\mathbf{e} \cdot \mathbf{q}(\mathbf{k})] \int \frac{d^3k}{(2\pi)^3} \exp(-i\mathbf{k}\mathbf{x}) \quad (15)$$

The decomposition of the projected field $\kappa(\theta)$ into spherical harmonics $Y_{\ell m}(\theta)$ is:

$$\kappa(\theta) = \sum_{\ell=0}^{\infty} \sum_{m=-\ell}^{+\ell} \kappa_{\ell m} Y_{\ell m}(\theta) \leftrightarrow \kappa_{\ell m} = \int_{4\pi} d\Omega \kappa(\theta) Y_{\ell m}^*(\theta) \quad (16)$$

$$Y_{\ell m}(\theta) = \sqrt{\frac{2\ell+1}{4\pi}} \sqrt{\frac{(\ell-|m|)!}{(\ell+|m|)!}} P_{\ell m}(\cos\theta) \exp(im\phi). \quad (17)$$

In the random phase approximation, one obtains for the variance $\langle |\kappa_{\ell m}|^2 \rangle$ of $\kappa(\theta)$ in two directions \mathbf{e}_1 and \mathbf{e}_2 :

$$\begin{aligned} \langle |\kappa_{\ell m}|^2 \rangle &= \int_0^{w_{\max}} dw_1 W(w_1) \int_{4\pi} d\Omega_1 Y_{\ell m}(\mathbf{e}_1) \\ &\int_0^{w_{\max}} dw_2 W(w_2) \int_{4\pi} d\Omega_2 Y_{\ell m}^*(\mathbf{e}_2) \\ &\int \frac{d^3k}{(2\pi)^3} \exp(-i\mathbf{k}\mathbf{e}_1 w_1) \exp(i\mathbf{k}\mathbf{e}_2 w_2) \langle [\mathbf{e}_1 \cdot \mathbf{q}(\mathbf{k})] [\mathbf{e}_2 \cdot \mathbf{q}^*(\mathbf{k})] \rangle. \end{aligned} \quad (18)$$

According to the cosmological principle, there is no preferred orientation, which allows to replace $\langle |a_{\ell m}|^2 \rangle$ with its average value over all m for a given ℓ :

$$C_{\kappa}(\ell) = \frac{1}{2\ell+1} \sum_{m=-\ell}^{+\ell} \langle |\kappa_{\ell m}|^2 \rangle. \quad (19)$$

The vector field $\mathbf{q}(\mathbf{k})$ can be separated into components parallel and perpendicular to the line-of-sight \mathbf{e} :

$$\mathbf{q} = \mathbf{q}_{\parallel} + \mathbf{q}_{\perp} \text{ with } \mathbf{q}_{\parallel} = \mathbf{e}(\mathbf{e} \cdot \mathbf{q}) \text{ and } \mathbf{q}_{\perp} = \mathbf{q} - \mathbf{q}_{\parallel} = \mathbf{e} \times (\mathbf{q} \times \mathbf{e}). \quad (20)$$

For the projections $\mathbf{e} \cdot \mathbf{q}_{\perp} = 0$ and $\mathbf{e} \times \mathbf{q}_{\parallel} = 0$ are valid. Eqn. (19) is further simplified by choosing the coordinate system in a way that the z -coordinate is parallel to the wave vector, $\mathbf{e}_z \parallel \mathbf{k}$. Introducing spherical coordinates (θ, ϕ) and putting $x = \cos\theta$ on obtains:

$$\mathbf{q}_{\parallel} \cdot \frac{\mathbf{k}}{k} = x q_{\parallel} \text{ and } \mathbf{q}_{\perp} \cdot \frac{\mathbf{k}}{k} = \sqrt{1-x^2} \exp(-i\phi) q_{\perp} \quad (21)$$

Furthermore, with $\exp(i\mathbf{k}\mathbf{e}w) = \exp(ikxw)$, the expression for the correlator is separated into:

$$\begin{aligned} \langle \mathbf{q}(\mathbf{k}) \cdot \mathbf{q}^*(\mathbf{k}) \rangle &= \\ x_1 x_2 \langle q_{\parallel}(\mathbf{k}) \cdot q_{\parallel}^*(\mathbf{k}) \rangle &+ \sqrt{1-x_1^2} e^{-i\phi_1} \sqrt{1-x_2^2} e^{i\phi_2} \langle q_{\perp}(\mathbf{k}) q_{\perp}^*(\mathbf{k}) \rangle. \end{aligned} \quad (22)$$

With these simplifications, the integrals over the azimuthal angles ϕ_1 and ϕ_2 in eqn. (19) can be carried out. Inserting the orthonormality relation $\int_0^{2\pi} d\phi \exp[i(n-m)\phi] = 2\pi\delta_{nm}$ reduces the summation over m to a single term, which is $m=0$ for the components parallel to the line-of-sight and $|m|=1$ for the components perpendicular to the line-of-sight. The final expression for the power spectrum $C_{\kappa}(\ell)$ is now split into the two orthogonal projections:

$$C_{\kappa}(\ell) = C_{\kappa}^{\parallel}(\ell) + C_{\kappa}^{\perp}(\ell). \quad (23)$$

2.3.1 Components parallel to the line-of-sight $C_{\kappa}^{\parallel}(\ell)$

For the power spectrum $C_{\kappa}^{\parallel}(\ell)$ of the components of \mathbf{q}_{\parallel} parallel to the line-of-sight, one obtains:

$$\begin{aligned} C_{\kappa}^{\parallel}(\ell) &= \frac{2}{(2\pi)^2} \int dk k^2 \int_0^{w_{\max}} dw_1 W(w_1) \int_0^{w_{\max}} dw_2 W(w_2) \\ &\int_{-1}^{+1} dx_1 \exp(-ikx_1 w_1) \int_{-1}^{+1} dx_2 \exp(ikx_2 w_2) \\ &[x_1 P_{\ell 0}(x_1) x_2 P_{\ell 0}(x_2)] \langle q_{\parallel}(\mathbf{k}, w_1) q_{\parallel}^*(\mathbf{k}, w_2) \rangle. \end{aligned} \quad (24)$$

The dx_1 - and dx_2 -integrations can be performed by taking advantage of the connection between Bessel functions and Legendre polynomials (Watson 1952; Abramowitz & Stegun 1972):

$$J_{\ell}(z) = \frac{1}{2i^{\ell}} \int_{-1}^{+1} dx P_{\ell}(x) \exp(izx), \quad (25)$$

which can be generalised to give:

$$\int_{-1}^{+1} dx x^n P_{\ell}(x) \exp(izx) = \frac{1}{i^n} \frac{d^n}{dz^n} J_{\ell}(z). \quad (26)$$

Inserting formula (26) for $n=1$ yields the final result:

$$\begin{aligned} C_{\kappa}^{\parallel}(\ell) &= \frac{1}{(2\pi)^2} \int dk \int_0^{w_{\max}} dw_1 W(w_1) \int_0^{w_{\max}} dw_2 W(w_2) \\ &\left[\frac{d}{dw_1} J_{\ell}(kw_1) \right] \left[\frac{d}{dw_2} J_{\ell}(kw_2) \right] \langle q_{\parallel}(\mathbf{k}, w_1) q_{\parallel}^*(\mathbf{k}, w_2) \rangle. \end{aligned} \quad (27)$$

2.3.2 Components perpendicular to the line-of-sight $C_{\kappa}^{\perp}(\ell)$

After reducing the summation to $|m|=1$, the power spectrum $C_{\kappa}^{\perp}(\ell)$ of the components of \mathbf{q}_{\perp} perpendicular to the line-of-sight reads:

$$\begin{aligned} C_{\kappa}^{\perp}(\ell) &= \frac{1}{(2\pi)^2 \ell(\ell+1)} \int dk k^2 \int_0^{w_{\max}} dw_1 W(w_1) \int_0^{w_{\max}} dw_2 W(w_2) \\ &\int_{-1}^{+1} dx_1 \exp(-ikx_1 w_1) \int_{-1}^{+1} dx_2 \exp(ikx_2 w_2) \\ &\left[\sqrt{1-x_1^2} P_{\ell 1}(x_1) \sqrt{1-x_2^2} P_{\ell 1}(x_2) \right] \langle q_{\perp}(\mathbf{k}, w_1) q_{\perp}^*(\mathbf{k}, w_2) \rangle. \end{aligned}$$

The integration over the polar angles x_1 and x_2 is slightly more complicated than the previous case. Inserting the definition of the associated Legendre polynomials $P_{\ell m}$ for $m=1$ gives another factor of $\sqrt{1-x^2}$:

$$P_{\ell m}(x) = (-1)^m (1-x^2)^{\frac{m}{2}} \frac{d^m P_{\ell}(x)}{dx^m} \rightarrow P_{\ell 1}(x) = -\sqrt{1-x^2} \frac{dP_{\ell}(x)}{dx}. \quad (28)$$

The derivative of the Legendre polynomial can be replaced via

$$(1-x^2) \frac{d}{dx} P_{\ell}(x) = \ell [P_{\ell-1}(x) - x P_{\ell}(x)], \quad (29)$$

and the integration be carried out by inserting relation (26). Then, the two Bessel functions can be combined by using the Bessel function's derivative relation:

$$\frac{d}{dz} [z^{\ell} J_{\ell}(z)] = z^{\ell} J_{\ell-1}(z) \rightarrow \frac{J_{\ell}(z)}{z} = \frac{1}{\ell} \left[J_{\ell-1} - \frac{d}{dz} J_{\ell}(z) \right], \quad (30)$$

which yields the formula:

$$\int_{-1}^{+1} dx \sqrt{1-x^2} P_{\ell 1}(x) \exp(izx) = \ell(\ell+1) \frac{J_{\ell}(z)}{z}. \quad (31)$$

This relation allows the final result to be written as:

$$\begin{aligned} C_{\kappa}^{\perp}(\ell) &= \frac{\ell(\ell+1)}{(2\pi)^2} \int dk \int_0^{w_{\max}} dw_1 W(w_1) \int_0^{w_{\max}} dw_2 W(w_2) \\ &\left[\frac{J_{\ell}(kw_1)}{w_1} \frac{J_{\ell}(kw_2)}{w_2} \right] \langle q_{\perp}(\mathbf{k}, w_1) q_{\perp}^*(\mathbf{k}, w_2) \rangle. \end{aligned} \quad (32)$$

3 GRAVITOMAGNETIC LENSING

3.1 Definitions

Light propagation through a slowly moving perfect fluid can be described by an effective refractive index n_{eff} which follows from the post-Newtonian expansion of the Raychaudhuri-equation to second order for a weakly perturbed space-time (Schneider et al. 1992):

$$n_{\text{eff}} = 1 - \frac{2}{c^2}\Phi + \frac{4}{c^3}\mathbf{A} \cdot \mathbf{e}. \quad (33)$$

Here, Φ is the scalar potential and \mathbf{A} are the gravitomagnetic vector potentials. \mathbf{e} denotes a unit tangent vector along the photon geodesic. In this approximation, the metric takes account of the matter density ρ and the matter current densities $\mathbf{j} = \rho\mathbf{v}$ (i.e. terms of order v/c), but neglects the stresses $T_{ij} = \rho v_i v_j + p\delta_{ij}$. The smallness of these terms (being of order v^2/c^2) makes them unobservable, but they would be sensitive to the velocity tensor $v_i v_j$, i.e. to shear flows, velocity dispersions and turbulence.

In the near zone of a system of slowly moving bodies the retardation can be neglected; in this case the expressions for Φ and \mathbf{A} are given as solutions to Laplace's equation:

$$\Delta\Phi(\mathbf{r}) = 4\pi G\rho(\mathbf{r}) \quad \leftrightarrow \quad \Phi(\mathbf{r}) = -G \int d^3r' \frac{\rho(\mathbf{r}')}{|\mathbf{r} - \mathbf{r}'|} \quad (34)$$

$$\Delta\mathbf{A}(\mathbf{r}) = 4\pi G\mathbf{j}(\mathbf{r}) \quad \leftrightarrow \quad \mathbf{A}(\mathbf{r}) = -G \int d^3r' \frac{\mathbf{j}(\mathbf{r}')}{|\mathbf{r} - \mathbf{r}'|}. \quad (35)$$

The dark matter flux \mathbf{j} is defined as the momentum density $\mathbf{j} \equiv \rho\mathbf{v}$.

An expression for $d\mathbf{e}/dw$, i.e. the change in propagation direction, follows from the variational principle $\delta \int ds n_{\text{eff}} = 0$. s denotes an affine parameter. The deflection angle α , being defined as $\alpha = \mathbf{e}_{\text{initial}} - \mathbf{e}_{\text{final}}$ can be obtained by integration:

$$\alpha = \frac{2}{c^2} \int ds \nabla_{\perp} \Phi - \frac{4}{c^3} \int ds \mathbf{e} \times \text{rot} \mathbf{A}. \quad (36)$$

The derivative perpendicular to the line-of-sight is defined via $\nabla_{\perp} \Phi \equiv \nabla \Phi - \mathbf{e}(\mathbf{e} \cdot \nabla \Phi)$. The first contribution to α in eqn. (36) corresponds to the attraction \mathbf{g} towards the deflecting mass via $\mathbf{g} = -\nabla \Phi$.

The second term, however, is due to the gravitomagnetic fields generated by the matter current densities \mathbf{j} . This contribution is related to the dragging of inertial frames which gives rise to the precession of orbiting spinning tops in the particular case of rotation of the field-generating body (Lense-Thirring precession, to be measured by Gravity Probe B²). This formalism has been applied to various astrophysical systems, namely by Ibanez (1983) to gravitational light deflection of a rotating galaxy and by Sereno (2003), who considered light deflection on rotating stars. Furthermore, corrections to the deflection angle in galactic microlensing due to moving lenses have been evaluated by Heyrovsky (2004).

3.2 Gravitomagnetic lensing by the large-scale structure

Adopting the Born-approximation, which states that the gravitational light deflection is weak such that the integral in eqn. (36) can be evaluated along a straight line instead of the photon geodesic itself, it can be seen that gravitational lensing is insensitive to derivatives of the potentials along the line-of-sight. Working out the deflection angles α and the tidal matrix $\psi_{ij} = \partial\alpha_i/\partial x_j$ while neglecting derivatives along the line-of-sight yields formulae analogous to the case of static lensing, but with the gravitational potential Φ replaced by $\Phi - \frac{2}{c}A_{\parallel}$. Thus, the sources of gravitational light deflection

are the matter distribution δ and the component of the matter flux j_{\parallel} parallel to the line-of-sight. The gravitational light deflection is stronger, if an object is moving towards the observer, because the photon stays in the interaction potential for a longer period of time, and vice versa.

With the source term $\delta + \frac{2}{c}j_{\parallel}$, one obtains for the lensing convergence κ up to the comoving distance w (Bartelmann & Schneider 2001):

$$\kappa(\boldsymbol{\theta}, w) = \frac{3H_0^2\Omega_0}{2c^2} \int_0^w dw' \frac{f_K(w')f_K(w_{\text{max}} - w')}{f_K(w_{\text{max}})a(w')} \left(\delta + \frac{2}{c}j_{\parallel} \right). \quad (37)$$

where $f_K(w) = w$, if spatial hypersurfaces are flat, which is the case for $\Omega_M + \Omega_{\Lambda} = 1$. The redshift distribution of lensed population of background sources such as faint blue galaxies is described by the distribution $p(z)dz$, being recast in comoving distance, $Z(w)dw = p(z)dz$. Then, the average influence $\bar{Z}(w)$ of the lever arms of the optical path for a given configuration of source and lens is given by:

$$\bar{Z}(w) = \int_w^{w_{\text{max}}} dw' Z(w') \frac{f_K(w' - w)}{f_K(w')}. \quad (38)$$

In this work, we assume the generic distribution in redshift z for faint blue galaxies (c.f. Ellis 1997),

$$p(z)dz = p_0 z^2 \exp(-z^{\beta}) \text{ with } \frac{1}{p_0} = \frac{1}{\beta} \Gamma\left(\frac{3}{\beta}\right). \quad (39)$$

with mean redshift $\langle z \rangle = \Gamma(4/\beta)/\Gamma(3/\beta) \simeq 1.5$ and most likely redshift $z_{\text{max}} = (2/\beta)^{1/\beta} \simeq 1.21$ for $\beta = 3/2$. For the average convergence $\bar{\kappa}$, the final result reads:

$$\begin{aligned} \bar{\kappa}(\boldsymbol{\theta}) &= \int_0^{w_{\text{max}}} dw Z(w) \kappa(\boldsymbol{\theta}, w) \\ &= \frac{3H_0^2\Omega_0}{2c^2} \int_0^{w_{\text{max}}} dw \bar{Z}(w) \frac{f_K(w)}{a(w)} \left(\delta + \frac{2}{c}j_{\parallel} \right). \end{aligned} \quad (40)$$

For $\bar{Z}(w)$, the phenomenological fitting formula

$$\bar{Z}(w) \simeq Z_0 \exp\left(-\frac{1}{1 - [\log(w/w_0)]^b}\right), \quad (41)$$

with $Z_0 = 1.441$, $b = 3.186$ and $w_0 = 2314 \text{ Mpc}/h$ is used, which yields excellent agreement with the properly evaluated function, as shown by Fig. 1. The fitting formula alleviates the need of numerically carrying out the integration in eqn. (38) when projecting the dark matter power spectrum.

3.3 Perturbative treatment

When considering gravitomagnetic corrections to gravitational lensing, the source term δ of static lensing has to be replaced by $q_{\parallel} = (1 + \frac{2}{c}v_{\parallel})\delta$. It should be emphasised, that the fluctuations in a weak lensing shear field are predominantly caused by modes in k -space, that are propagating perpendicularly to the line-of-sight (Blandford et al. 1991). Evaluating the correlator $\langle q_{\perp}(\mathbf{k}, w_1)q_{\perp}(\mathbf{k}, w_2) \rangle$ yields apart from the dominating 2-point term,

$$\langle q_{\perp}(\mathbf{k}, w_1)q_{\perp}(\mathbf{k}, w_2) \rangle_{2\text{pt}} = D(w_1)D(w_2)\langle \delta(\mathbf{k})\delta^*(\mathbf{k}) \rangle, \quad (42)$$

contributions of 3- and 4-point terms. The 2-point term stated in eqn. (42) is of order unity and is the basis of the conventional theory of static gravitational lensing. In the perturbative treatment, the coupling of \mathbf{k} -modes in nonlinear structure growth is neglected, integrations are implicitly taken to be restricted to quasi-linear scales.

² <http://www.gravityprobeb.com>

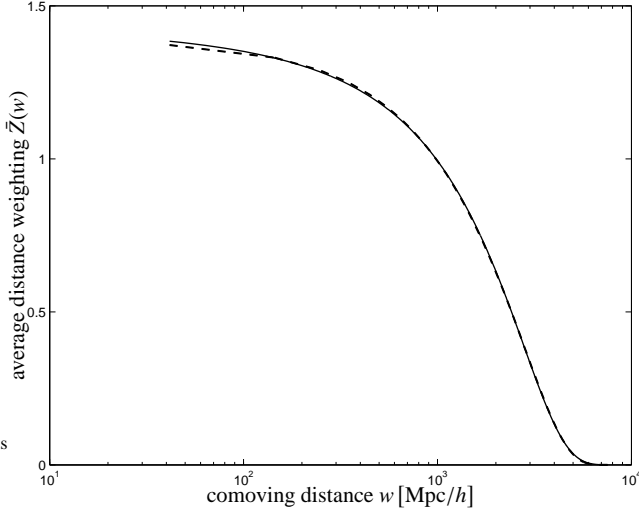


Figure 1. The redshift weighting function $\bar{Z}(w)$ (c.f. eqn. (38), rendered as a dashed line), and the fitting formula (41) (solid line) in comparison.

3.3.1 3-point term

The 3-point term $\langle q_{\perp}(\mathbf{k}, w_1) q_{\perp}^*(\mathbf{k}, w_2) \rangle_{3\text{pt}}$ consists of four contributions and is of order v/c compared to the 2-point term (c.f. eqn. (42)):

$$\langle q_{\perp}(\mathbf{k}, w_1) q_{\perp}^*(\mathbf{k}, w_2) \rangle_{3\text{pt}} = \frac{1}{c} \int \frac{d^3 p}{(2\pi)^3} \left\{ \quad (43)$$

$$\begin{aligned} & \langle \delta(-\mathbf{k}, w_1) v_{\perp}(\mathbf{p}, w_2) \delta(\mathbf{k} - \mathbf{p}, w_2) \rangle + \langle \delta(-\mathbf{k}, w_1) v_{\perp}(\mathbf{k} - \mathbf{p}, w_2) \delta(\mathbf{p}, w_2) \rangle + \\ & \langle \delta(\mathbf{k}, w_2) v_{\perp}(-\mathbf{p}, w_1) \delta(\mathbf{p} - \mathbf{k}, w_1) \rangle + \langle \delta(\mathbf{k}, w_2) v_{\perp}(\mathbf{p} - \mathbf{k}, w_1) \delta(-\mathbf{p}, w_1) \rangle \end{aligned} \left. \right\}$$

Here, the relations $\delta^*(\mathbf{k}) = \delta(-\mathbf{k})$ and $\mathbf{v}^*(\mathbf{k}) = \mathbf{v}(-\mathbf{k})$ were inserted, which hold for real fields. By using this fact, the condition $\sum_i \mathbf{k}_i = \mathbf{0}$ is fulfilled which allows the 3-point correlators in eqn. (43) to be reduced to products of 2-point correlators by virtue of the formulae derived in Appendix A. This yields four terms of the type $\langle v_{\perp} \delta \rangle / c$ and two contributions $\langle v_{\perp} \delta \rangle^2 / c^2$ of second order.

The correlation function can then be projected onto a plane perpendicular to wave vector \mathbf{k} : The component of the velocity in the celestial plane is given by $\mathbf{v}_{\perp} = \mathbf{k} \times (\mathbf{v} \times \mathbf{k}) / k^2$ and hence $v_{\perp} = v \sin \theta = v \sqrt{1 - x^2}$, with $x = \cos \theta$, where θ is the angle of separation between \mathbf{p} and \mathbf{k} . In doing this, the contributions of the type $\langle v_{\perp} \delta \rangle^2 / c^2$ vanish because they contain a multiplicative term $\langle \delta(\mathbf{k}) \mathbf{v}(\mathbf{k}) \rangle$, which is a vector field collinear to \mathbf{k} . The remaining terms can be combined to give:

$$\begin{aligned} (2\pi)^3 \langle q_{\perp}(\mathbf{k}, w_1) q_{\perp}^*(\mathbf{k}, w_2) \rangle_{3\text{pt}} &= \frac{4\pi}{c} D(w_1) D(w_2) [g'(w_1) + g'(w_2)] \\ & \int p^2 dp \int_{-1}^{+1} dx \sqrt{1 - x^2} \left\{ P(|\mathbf{p}|) P(|\mathbf{p} - \mathbf{k}|) M(\mathbf{p}, \mathbf{p} - \mathbf{k}) \left[\frac{1}{|\mathbf{p}|} + \frac{p}{|\mathbf{p} - \mathbf{k}|^2} \right] \right. \\ & \left. + P(|\mathbf{k}|) \left[M(\mathbf{k}, -\mathbf{p}) \frac{P(|\mathbf{p}|)}{|\mathbf{p}|} + M(\mathbf{k}, \mathbf{p} - \mathbf{k}) \frac{p}{|\mathbf{p} - \mathbf{k}|^2} P(|\mathbf{p} - \mathbf{k}|) \right] \right\} \quad (44) \end{aligned}$$

In the integrand of eqn. (44), the replacement $|\mathbf{p} - \mathbf{k}|^2 = k^2 - 2kpx + p^2$ can be inserted. Additionally, the time evolution of the velocity-density cross correlation function,

$$\langle v_{\perp}(\mathbf{k}, w_1) \delta^*(\mathbf{k}, w_2) \rangle = g'(w_1) D(w_2) \langle v_{\perp}(\mathbf{k}) \delta^*(\mathbf{k}) \rangle, \quad (45)$$

was inserted. The function $M(\mathbf{p}, \mathbf{p}')$ is defined as:

$$M(\mathbf{p}, \mathbf{p}') = \frac{10}{7} + \frac{\mathbf{p}\mathbf{p}'}{p p'} \left(\frac{p}{p'} + \frac{p'}{p} \right) + \frac{4}{7} \left(\frac{\mathbf{p}\mathbf{p}'}{p p'} \right)^2. \quad (46)$$

It should be emphasised, that this 3-point correlator does not take account of the evolution of non-Gaussian features in the correlation function $\langle \delta(\mathbf{k}_1) \delta(\mathbf{k}_2) \delta(\mathbf{k}_3) \rangle$ and their influence on lensing determined by Jain & Seljak (1997); Bernardeau (1997) and Takada & Jain (2003a,b), which strongly affects weak lensing quantities on small angular scales.

3.3.2 4-point term

The last contribution to the weak lensing power spectrum evoked by gravitomagnetic corrections is the 4-point term $\langle q_{\perp}(\mathbf{k}, w_1) q_{\perp}^*(\mathbf{k}, w_2) \rangle_{4\text{pt}}$, which is of order v^2/c^2 and thus strongly suppressed. The derivation of the term is easy prey: It can be done in complete analogy to that of the Ostriker-Vishniac effect (Ostriker & Vishniac 1986; Vishniac 1987), where any optical depth depending on redshift needs to be replaced by the appropriate weighting function (c.f. Sect. 4.6) and conversions from dark matter densities into baryonic densities are to be discarded.

The derivation evolves cross-terms between the velocity and density fields, perhaps the most elegant way of reducing it to a sum of 2-point correlations is given by Ma & Fry (2002), using a result from Monin & Yaglom (1965a,b):

$$\begin{aligned} (2\pi)^3 \langle q_i(\mathbf{k}) q_j^*(\mathbf{k}) \rangle_{4\text{pt}} &\equiv P_{qq}^{ij}(|\mathbf{k}|) \simeq \\ & \frac{4}{c^2} \int \frac{d^3 p}{(2\pi)^3} \int \frac{d^3 p'}{(2\pi)^3} (2\pi)^3 \delta_D(\mathbf{k} - \mathbf{p} - \mathbf{p}') \\ & \times \left[\frac{p^i}{|\mathbf{p}^i|} \frac{p^j}{|\mathbf{p}^j|} P_{vv}(|\mathbf{p}|) P_{\delta\delta}(|\mathbf{p}'|) + \frac{p^i}{|\mathbf{p}^i|} \frac{p'^j}{|\mathbf{p}'^j|} P_{\delta v}(|\mathbf{p}|) P_{\delta v}(|\mathbf{p}'|) \right], \quad (47) \end{aligned}$$

where the irreducible 4-point correlation $P_{\delta v \delta v}(\mathbf{k})$ has been neglected.

Following Ma & Fry (2002), the projection to be carried out is $(2\pi)^3 \langle q_{\perp}(\mathbf{k}) q_{\perp}^*(\mathbf{k}) \rangle_{4\text{pt}} = 2 \sum_{ij} \mathbf{e}_i \mathbf{e}_j P_{qq}^{ij}(|\mathbf{k}|)$, where \mathbf{e}_i and \mathbf{e}_j are unit vectors along the lines-of-sight. The expression for $P_{qq}^{ij}(|\mathbf{k}|)$ is given by eqn. (47). In neglecting the irreducible 4-point term one obtains:

$$\begin{aligned} (2\pi)^3 \langle q_{\perp}(\mathbf{k}) q_{\perp}^*(\mathbf{k}) \rangle_{4\text{pt}} &= \frac{1}{c^2} \int \frac{d^3 p}{(2\pi)^3} \left\{ \quad (48) \\ & (1 - x^2) P_{\delta\delta}(|\mathbf{k} - \mathbf{p}|) P_{vv}(|\mathbf{p}|) - \frac{(1 - x^2)p}{|\mathbf{k} - \mathbf{p}|} P_{\delta v}(|\mathbf{k} - \mathbf{p}|) P_{\delta v}(|\mathbf{p}|) \right\} \end{aligned}$$

Inserting the time-evolution of the density-velocity and velocity-velocity cross correlation terms,

$$\langle v_{\perp}(\mathbf{k}, w_1) v_{\perp}^*(\mathbf{k}, w_2) \rangle = g'(w_1) g'(w_2) \langle v_{\perp}(\mathbf{k}) v_{\perp}^*(\mathbf{k}) \rangle, \quad (49)$$

$$\langle v_{\perp}(\mathbf{k}, w_1) \delta^*(\mathbf{k}, w_2) \rangle = g'(w_1) D(w_2) \langle v_{\perp}(\mathbf{k}) \delta^*(\mathbf{k}) \rangle, \quad (50)$$

yields the final result:

$$\begin{aligned} (2\pi)^3 \langle q_{\perp}(\mathbf{k}, w_1) q_{\perp}^*(\mathbf{k}, w_2) \rangle_{4\text{pt}} &= 4D(w_1) D(w_2) g'(w_1) g'(w_2) \times \\ & \frac{2\pi}{c^2} \int dp \int_{-1}^{+1} dx P(|\mathbf{k} - \mathbf{p}|) P(|\mathbf{p}|) \frac{k(1 - x^2)(k - 2xp)}{k^2 - 2xkp + p^2}. \quad (51) \end{aligned}$$

3.4 Corrections to the power spectrum

The three-dimensional power spectra $\langle q_{\perp}(\mathbf{k}) q_{\perp}^*(\mathbf{k}) \rangle$ of the matter currents parallel to the line-of-sight is shown in Fig. 2 for the various n -point contributions. Compared to the dominating 2-point

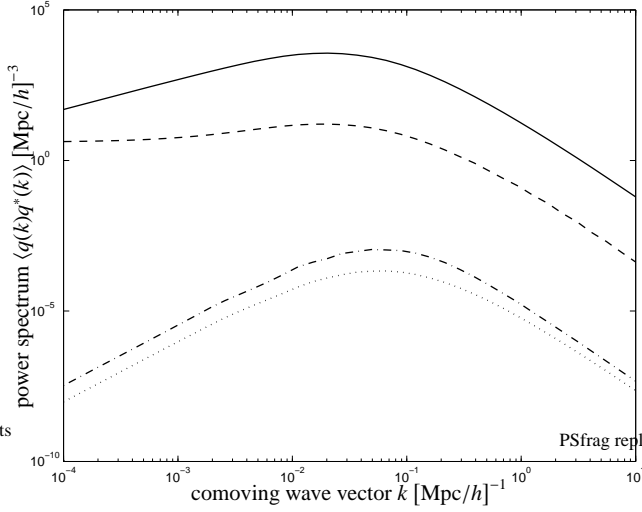


Figure 2. Three-dimensional power spectrum $\langle q_{\perp}(k)q_{\perp}^*(k) \rangle$ including dark matter currents perpendicular to the line-of-sight, split up into the 2-point contribution (solid line), the 3-point contribution (dashed line) and the 4-point contribution (dash-dotted line). Additionally, the 4-point term of the currents parallel to the line-of-sight $\langle q_{\parallel}(k)q_{\parallel}^*(k) \rangle$ is drawn (dotted line). The power spectra are given for the present epoch, i.e. $a = 1$ and $z = 0$.

term, the 3-point term is smaller by more than two orders of magnitude on small scales, but it becomes important on large spatial scales beyond 1 Gpc where it levels out. On these large scales, however, limitations due to cosmic variance and insufficient sampling due to galactic foregrounds cast doubt on its detectability. The leveling on large spatial scales of the 3-point term is due to the fact, that for small k all powers in p in eqn. (44) add up to zero, which results in a flat curve for $\langle q_{\perp}(k)q_{\perp}^*(k) \rangle_{3\text{pt}}$. In comparison to the 3-point term, the 4-point term is smaller by another three orders of magnitude, but in shape it very much resembles the 2-point term and its influence on the weak lensing power spectrum is safely negligible.

3.5 Projected lensing power spectra

The final expression for $\langle q_{\perp}(k)q_{\perp}^*(k) \rangle$ can be projected by means of eqn. (32) to yield the angular power spectrum of any lensing quantity, for example the convergence κ . The distance weighting function to be employed can be read off from eqn. (40):

$$W_L(w) = \frac{3H_0^2\Omega_0}{2c^2} \frac{f_K(w)}{a(w)} \int_w^{w_{\max}} dw' Z(w') \frac{f_K(w' - w)}{f_K(w')}. \quad (52)$$

By substituting $y = kw$, the distance weighting $W_L(w)$ can be combined with the time evolution of the correlators to yield the functions

$$\varphi_{\ell}(k)_{2\text{pt}} = \left[\int_0^{y_{\max}} dy W_L \left(\frac{y}{k} \right) \frac{J_{\ell}(y)}{y} D(y) \right]^2, \quad (53)$$

$$\varphi_{\ell}(k)_{3\text{pt}} = \int_0^{y_{\max}} dy W_L \left(\frac{y}{k} \right) \frac{J_{\ell}(y)}{y} D(y) G(y) \int_0^{y_{\max}} dy W_L \left(\frac{y}{k} \right) \frac{J_{\ell}(y)}{y} D(y) \quad (54)$$

$$\varphi_{\ell}(k)_{4\text{pt}} = \left[\int_0^{y_{\max}} dy W_L \left(\frac{y}{k} \right) \frac{J_{\ell}(y)}{y} D(y) G(y) \right]^2, \quad (55)$$

which carry out the projection of the 3-dimensional power spectrum $\langle q_{\perp}(k)q_{\perp}^*(k) \rangle$ to the angular power spectrum $C_{\kappa}(\ell)$ by convolution:

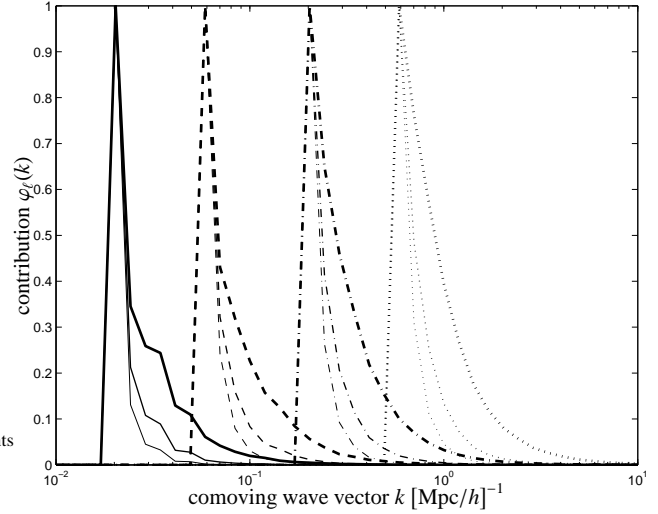


Figure 3. Contribution $\varphi_{\ell}(k)$ of the 2-point terms (thick lines), 3-point terms (medium lines) and 4-point terms (thin lines) to the angular power spectrum $C_{\kappa}(\ell)$ of the weak lensing convergence κ as a function of wave vector k , for $\ell = 100$ (solid line), $\ell = 300$ (dashed line), $\ell = 1000$ (dash-dotted line) and $\ell = 3000$ (dotted line). The curves are normalised to unity.

$$C_{\kappa}(\ell) = \frac{1}{(2\pi)^2} \ell(\ell + 1) \int dk \langle q_{\perp}(k)q_{\perp}^*(k) \rangle \times \varphi_{\ell}(k), \quad (56)$$

where the associativity of the time-evolution enables the 3-fold integration in eqn. (32) to be reduced to a 2-fold integration.

The functions $\varphi_{\ell}(k)_{2\text{pt}}$, $\varphi_{\ell}(k)_{3\text{pt}}$ and $\varphi_{\ell}(k)_{4\text{pt}}$ are shown in Fig. 3. Clearly, the fluctuations on a certain angular scale described by the angular power spectrum $C(\ell)$ are dominated by spatial fluctuations with a certain wave vector k , which leads the peak of the function $\varphi_{\ell}(k)$ to shift with increasing ℓ . The projection kernels $\varphi_{\ell}(k)$ for the different n -point correlation functions show the common feature of rising fast at small k , but their decays at large k vary appreciably, because the increasing influence of the time evolution of the velocities $G(w)$ makes the functions to drop faster with increasing values of k . In this way, the observed asymptotic behaviour is $\varphi_{\ell}(k_{2\text{pt}}) \propto k^{-2}$ for the 2-point projector, but the $\varphi_{\ell}(k_{3\text{pt}})$ and $\varphi_{\ell}(k_{4\text{pt}})$ exhibit faster decays that are not described by a mere power law.

The angular power spectrum of the weak lensing convergence $C_{\kappa}(\ell)$ and its corrections due to gravitomagnetic terms is depicted in Fig. 4. Even at the largest angular scales considered here, the function $\varphi_{\ell}(k)$ peaks at values of k at which the corrections of the 3-point term are negligible. The detection of corrections to the weak lensing power spectrum due to gravitomagnetic terms requires the measurement of weak lensing shear on very large angular scales, which is beyond feasibility with current technology. On large angular scales, cosmic variance additionally limits the observability of gravitomagnetic lensing.

4 INTEGRATED SACHS-WOLFE EFFECT

4.1 Definitions

The growth of structure imprints additional anisotropies on the cosmic microwave background (CMB) by the time variation of the gravitational potentials along the propagation path of a CMB photon. This effect is called the integrated Sachs-Wolfe (ISW) effect in the regime of linear structure formation (Sachs & Wolfe 1967; Hu & Sugiyama 1994) and Rees-Sciama effect (Rees & Sciama

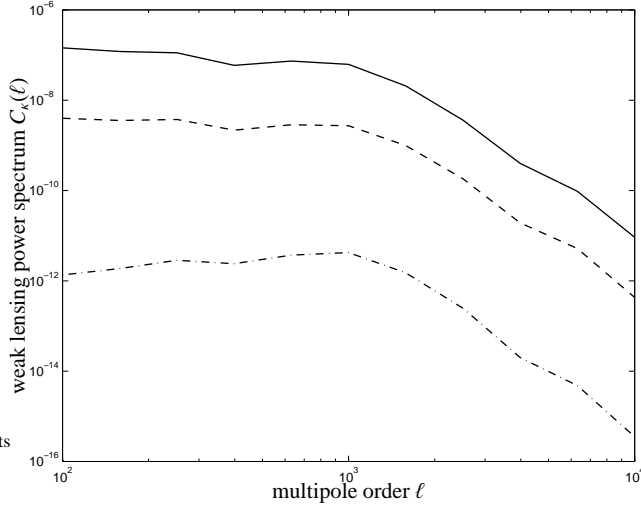


Figure 4. Angular power spectrum $C_\kappa(\ell)$ of the weak lensing convergence κ and its correction due to gravitomagnetic potentials. The contributions from the 2-point term (solid line), the 3-point term (dashed line) and the 4-point term (dash-dotted line) are given separately.

1968; Seljak 1996; Cooray 2002) if the density perturbations grow nonlinearly. The perturbations ΔT of the sky temperature T can be written as:

$$\tau \equiv \frac{\Delta T}{T} = -\frac{2}{c^3} \int dw \frac{\partial \Phi}{\partial t}, \quad (57)$$

where $\partial \Phi / \partial t$ is the derivative of the gravitational potentials with respect to conformal time t . Similar to gravitomagnetic lensing discussed in Sect. 3.1 (c.f. eqns. (33) and (36)), the effect is of the order $1/c^3$.

4.2 Connection to the gravitomagnetic potentials

Using the definition of $\Phi(\mathbf{r})$ and the equation of continuity, $\dot{\rho} + \text{div} \mathbf{j}$, where $\mathbf{j} = \rho \mathbf{v}$ is the matter current density, one obtains for the time derivative of Φ :

$$\frac{\partial}{\partial t} \Phi(\mathbf{r}, t) = -G \int d^3 r' \frac{\dot{\rho}(\mathbf{r}')}{|\mathbf{r} - \mathbf{r}'|} = G \int d^3 r' \frac{\nabla' \cdot \mathbf{j}(\mathbf{r}')}{|\mathbf{r} - \mathbf{r}'|}. \quad (58)$$

Integration by parts with respect to $d^3 r'$ yields:

$$G \int d^3 r' \frac{\nabla' \cdot \mathbf{j}(\mathbf{r}')}{|\mathbf{r} - \mathbf{r}'|} = -G \int d^3 r' \mathbf{j}(\mathbf{r}') \cdot \nabla' \frac{1}{|\mathbf{r} - \mathbf{r}'|}. \quad (59)$$

With the identity

$$\nabla' \frac{1}{|\mathbf{r} - \mathbf{r}'|} = -\nabla \frac{1}{|\mathbf{r} - \mathbf{r}'|}, \quad (60)$$

the derivative with respect to the primed coordinate can be replaced by a derivative with respect to the unprimed one. In the last steps, the ∇ -operator can be drawn in front of the integral and the definition of \mathbf{A} (c.f. eqn. (35)) be inserted to yield:

$$G \int d^3 r' \mathbf{j}(\mathbf{r}') \cdot \nabla \frac{1}{|\mathbf{r} - \mathbf{r}'|} = -\nabla \cdot \left(-G \int d^3 r' \frac{\mathbf{j}(\mathbf{r}')}{|\mathbf{r} - \mathbf{r}'|} \right) = -\text{div} \mathbf{A}. \quad (61)$$

Thus, the final result reads:

$$\frac{\partial}{\partial t} \Phi(\mathbf{r}, t) = -\text{div} \mathbf{A} \rightarrow \tau = \frac{2}{c^3} \int dw \text{div} \mathbf{A}. \quad (62)$$

Eqn. (62) has a lucid interpretation: The formation of objects such as clusters of galaxies requires the matter fluxes \mathbf{j} to converge and

to accumulate matter ($\dot{\rho} > 0$). Consequently, potential wells deepen and give rise to the iSW-effect in regions where $\text{div} \mathbf{A}$ does not vanish. The iSW-effect measures the rate of change of a potential with respect to conformal time, or equivalently, the divergence of the vector potential \mathbf{A} , which is proportional to the accretion rate in the Lagrangian frame.

4.3 Putting the Sachs-Wolfe effect in a cosmological context

In order to relate the statistical properties of the iSW temperature fluctuations $\tau(\boldsymbol{\theta})$ to those of the matter streams $\mathbf{j}(\mathbf{r})$, the auxiliary vector field $\boldsymbol{\chi}(\boldsymbol{\theta})$ is introduced, which is defined as the negative gradient of the iSW temperature fluctuation $\tau(\boldsymbol{\theta})$:

$$\boldsymbol{\chi}(\boldsymbol{\theta}) \equiv -\nabla \tau(\boldsymbol{\theta}), \quad (63)$$

i.e. $\boldsymbol{\chi}(\boldsymbol{\theta})$ points along the steepest descent in temperature from hot to cold patches in an iSW field. Inserting eqn. (62) into the defining equation for $\boldsymbol{\chi}(\boldsymbol{\theta})$ and converting the derivation with respect to the angular variable $\boldsymbol{\theta}$ into a derivation with respect to the comoving variable \mathbf{r} by using $\nabla_{\boldsymbol{\theta}} = f_K(w) \nabla$, enables interchanging integration and differentiation:

$$\boldsymbol{\chi}(\boldsymbol{\theta}) = \frac{2}{c^3} \int dw f_K(w) \nabla (\text{div} \mathbf{A}) = \frac{2}{c^3} \int dw f_K(w) \Delta \mathbf{A}. \quad (64)$$

Additionally, the replacement $\nabla (\text{div} \mathbf{A}) = \Delta \mathbf{A}$ is inserted, which is valid if $\text{rot} \text{rot} \mathbf{A} = \mathbf{0}$. This is fulfilled in vorticity-free velocity fields, $\text{rot} \mathbf{j} = \mathbf{0}$. In linear theory, initial vorticity perturbations are damped and after a sufficiently long time, the linear velocity field should be completely irrotational. Even in the regime of quasi- or nonlinear structure formation, Kelvin's circulation theorem forces the flow to remain irrotational and described by a velocity potential until dissipative processes on smallest scales give rise to vortical flows.

Inserting Laplace's equation in the comoving frame, $\Delta \mathbf{A} = 4\pi G a^2 \langle \rho \rangle (\delta \mathbf{v})$ with the source term $\mathbf{j} = \delta \mathbf{v}$, allows to replace Newton's constant G and the ambient mass density $\langle \rho \rangle$ by using $\rho_{\text{crit}} = 3H_0^2 / (8\pi G)$, $\langle \rho \rangle_0 = \Omega_0 \rho_{\text{crit}}$ and $\langle \rho \rangle = \langle \rho \rangle_0 / a^3$:

$$\boldsymbol{\chi}(\boldsymbol{\theta}) = \frac{2}{c^3} \int dw f_K(w) \frac{4\pi G \langle \rho \rangle}{a} \mathbf{j} = \frac{3H_0^2 \Omega_0}{c^2} \int dw \frac{f_K(w)}{a(w)} \frac{\mathbf{j}}{c}. \quad (65)$$

The structural similarity of eqn. (65) with the weak lensing convergence eqn. (40) is striking.

Now, the 2-point correlation of the iSW temperature gradient field $\boldsymbol{\chi}(\boldsymbol{\theta})$ is related to the matter flux density $\mathbf{j}(\mathbf{r})$. For the derivation of the correlation function $C_\tau(\ell)$ of the temperature field $\tau(\boldsymbol{\theta})$ itself, one rewrites eqn. (63) in Fourier space, yielding:

$$\boldsymbol{\chi}(\boldsymbol{\theta}) = \int \frac{d^2 \ell}{(2\pi)^2} \boldsymbol{\chi}(\boldsymbol{\ell}) \exp(i\boldsymbol{\ell} \cdot \boldsymbol{\theta}) \rightarrow \boldsymbol{\chi}(\boldsymbol{\ell}) = i\boldsymbol{\ell} \tau(\boldsymbol{\ell}) \quad (66)$$

The expansion into Fourier modes rather than spherical harmonics is permissible, because τ is expected to show fluctuations on small angular scales, so that τ can be considered on a plane locally tangential to the celestial sphere. Squaring immediately gives:

$$C_\chi(\ell) = \ell^2 C_\tau(\ell) \simeq \ell(\ell + 1) C_\tau(\ell), \quad (67)$$

where the last step is a valid approximation for small angular scales. The complementarity of gravitational lensing and the iSW-effect and the lensing counterparts of iSW quantities are illustrated in the flow chart Fig. 5.

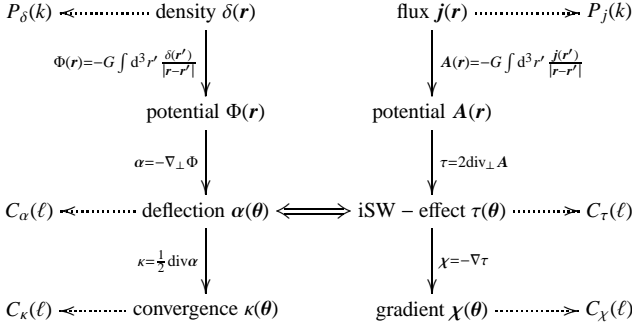


Figure 5. Flow chart with correspondent quantities in gravitational lensing (left column) and the integrated Sachs-Wolfe effect (right column). The quantity analogous to the iSW temperature fluctuation $\tau(\theta)$ in weak gravitational lensing is the deflection angle $\alpha(\theta)$.

4.4 Perturbative treatment

In the following we adopt the approximation that the rate of change of a potential is constant during the photon passage and that the accretion geometry does not change significantly. In this approximation, the component dA_z/dz of $\text{div} A$ is cancelled by the integration in eqn. (62) and makes the iSW effect to measure the components of $\text{div} A$ perpendicular to the line-of-sight, i.e. $\tau \propto \text{div}_\perp A = dA_x/dx + dA_y/dy$. Consequently, the matter fluxes $\mathbf{q}_\perp(\mathbf{x}) = \mathbf{j}_\perp(\mathbf{x})/c = \delta(\mathbf{x})\mathbf{v}_\perp(\mathbf{x})/c$ perpendicular to the line-of-sight primarily give rise to the iSW-effect. Accordingly, the fluctuations in the CMB due to the Rees-Sciama effect, being sensitive to the components of the matter flux perpendicular to the line-of-sight, are dominated by the components of k -modes parallel to the line of sight.

Power spectra of the form $\langle q_{\parallel}(\mathbf{k})q_{\parallel}^*(\mathbf{k}) \rangle$ have been considered by many authors in the derivation of the Ostriker-Vishniac effect (e.g. Vishniac 1987; Jaffe & Kamionkowski 1998). In order to obtain the projection onto the line-of-sight, $(2\pi)^3 \langle q_{\parallel}(\mathbf{k})q_{\parallel}^*(\mathbf{k}) \rangle_{4\text{pt}} = \sum_{ij} \frac{k_i^j}{|k^j|} \frac{k_j^i}{|k^i|} P_{qq}^{ij}(|\mathbf{k}|)$, has to be carried out, which can be interpreted as the quadratic form $\hat{\mathbf{k}}^T \tilde{P} \hat{\mathbf{k}}$ with a unit vector $\hat{\mathbf{k}}$ and the matrix $\tilde{P} = P_{qq}^{ij}$ (compare eqn. 47). The matrix \tilde{P} introducing the scalar product $\hat{\mathbf{k}}^T \tilde{P} \hat{\mathbf{k}}$ is positive definite, due to the reality of the density and velocity fields.

$$(2\pi)^3 \langle q_{\parallel}(\mathbf{k})q_{\parallel}^*(\mathbf{k}) \rangle_{4\text{pt}} = \quad (68)$$

$$\frac{4}{c^2} \int \frac{d^3 p}{(2\pi)^3} x^2 P_{\delta\delta}(|\mathbf{k}-\mathbf{p}|) P_{vv}(|\mathbf{p}|) + \frac{(k-p)x}{|\mathbf{k}-\mathbf{p}|} P_{\delta v}(|\mathbf{k}-\mathbf{p}|) P_{\delta v}(|\mathbf{p}|)$$

The scalar product $\mathbf{p}\mathbf{k}$ is again equal to pkx , where x is the cosine of the angle of separation. Inserting the velocity-density and velocity-velocity cross correlation functions with their proper time evolution,

$$\langle v_{\parallel}(\mathbf{k}, w_1) \delta^*(\mathbf{k}, w_2) \rangle = g'(w_1) D(w_2) \langle v_{\parallel}(\mathbf{k}) \delta^*(\mathbf{k}) \rangle, \quad (69)$$

$$\langle v_{\parallel}(\mathbf{k}, w_1) v_{\parallel}^*(\mathbf{k}, w_2) \rangle = g'(w_1) g'(w_2) \langle v_{\parallel}(\mathbf{k}) v_{\parallel}^*(\mathbf{k}) \rangle, \quad (70)$$

yields the final result:

$$(2\pi)^3 \langle q_{\parallel}(\mathbf{k}, w_1) q_{\parallel}(\mathbf{k}, w_2) \rangle_{4\text{pt}} = D(w_1) D(w_2) g'(w_1) g'(w_2) \times \frac{4}{c^2} \int d\mathbf{p} \int_{-1}^{+1} dx P(|\mathbf{k}-\mathbf{p}|) P(|\mathbf{p}|) \frac{kx(kx-2px^2+p)}{k^2-2kx+p^2}. \quad (71)$$

4.5 Power spectrum of dark matter currents

The three-dimensional power spectrum $\langle q_{\parallel}(\mathbf{k})q_{\parallel}^*(\mathbf{k}) \rangle$ of the matter currents perpendicular to the line-of-sight is given in Fig. 2. Its amplitude is by a factor of 4 smaller than the power spectrum $\langle q_{\perp}(\mathbf{k})q_{\perp}^*(\mathbf{k}) \rangle$, because the iSW-effect measures the streams δv in contrast to gravitomagnetic lensing, where the source terms read $(1+2v/c)\delta$. Despite the fact that different projections are considered, the shape and asymptotic forms of $\langle q_{\parallel}(\mathbf{k})q_{\parallel}^*(\mathbf{k}) \rangle$ and $\langle q_{\perp}(\mathbf{k})q_{\perp}^*(\mathbf{k}) \rangle$ are very similar.

4.6 integrated Sachs-Wolfe angular power spectrum

Fig. 7 shows the angular power spectra $C_\tau(\ell)$ of the iSW-effect $\tau(\theta)$ and $C_\chi(\ell)$ of the iSW temperature gradient $\chi(\theta)$ which have been obtained by applying the projection formula (27) to the spectrum $\langle q_{\parallel}(\mathbf{k})q_{\parallel}^*(\mathbf{k}) \rangle$ with the weighing function

$$W_{\text{iSW}}(w) = \frac{3H_0^2 \Omega_0 f_K(w)}{c^2 a(w)}, \quad (72)$$

which can be read off from eqn. (65). The redshift-weightings and the time-evolution of the density and velocity fields can be combined, which yields the function (73) after substituting $y = kw$,

$$\psi_\ell(k)_{4\text{pt}} = \left[\int_0^{y_{\text{max}}} dy W_{\text{iSW}} \left(\frac{y}{k} \right) \frac{dJ_\ell(y)}{dy} D(y) G(y) \right]^2 \quad (73)$$

which mediates between the 3-dimensional power spectrum $\langle q_{\parallel}(\mathbf{k})q_{\parallel}^*(\mathbf{k}) \rangle$ and the angular power spectrum $C_\tau(\ell)$ by convolution:

$$C_\tau(\ell) = \frac{1}{(2\pi)^2} \int dk \langle q_{\parallel}(\mathbf{k})q_{\parallel}^*(\mathbf{k}) \rangle \times \psi_\ell(k). \quad (74)$$

Again, the 3-fold integration in eqn. (27) is reduced to a 2-fold integration. The shape of the function $\psi_\ell(k)$ is depicted in Fig. 6 for various values of ℓ . In contrast to the function $\varphi_\ell(k)$ used in the projection of the lensing power spectra, the function $\psi_\ell(k)$ is symmetric about its peak, which is caused by the replacement of $J_\ell(y)/y$ with the derivative $dJ_\ell(y)/dy$. The fast variability is again due to the strong influence of the velocity time evolution $G(y)$.

The angular power spectrum $C_\tau(\ell)$ of the iSW temperature fluctuations $\tau(\theta)$ along with the primary CMB fluctuations and the limiting *Planck*-sensitivity is depicted in Fig. 7. The angular power spectrum has an amplitude of $\approx 3 \times 10^{-11} \text{ K}^2$ at small ℓ and shows a slow variation with the multipole order ℓ . The amplitude agrees well with the result from Seljak (1996), but the decline of the power spectrum on large angular scales could not be confirmed, which is due to the fact that for large angles, the Bessel functions $J_\ell(x)$ are a poor approximation to the Legendre polynomials $P_\ell(x)$. The position of the peak in the projection kernel $\psi_\ell(k)$ suggests that on the largest scales considered here, the angular spectrum $C_\tau(\ell)$ is dominated by fluctuations at the maximum of $P(k)$ on scales at $k^{-1} \approx 10 \text{ Mpc}$. With increasing multipole order ℓ , the peak in $\psi_\ell(k)$ shifts only slowly towards higher values of k , which explains the small variation of $C_\chi(\ell) = \ell(\ell+1)C_\tau(\ell)$.

The channel averaged *Planck*-sensitivity is described by (Knox 1995; Tegmark & Efstathiou 1996):

$$C_{\text{noise}}(\ell) = \frac{4\pi\sigma^2}{N_{\text{pix}}} \exp[\theta_b^2 \ell(\ell+1)], \quad (75)$$

where $N_{\text{pix}} \approx 5.03 \times 10^7$ is the number of pixels and θ_b the FWHM extension of the *Planck*-beam. For the average amplitude of the noise σ_{eff} per solid angle subtended by a single pixel we use the quadratic harmonic mean over all *HFI*-channels:

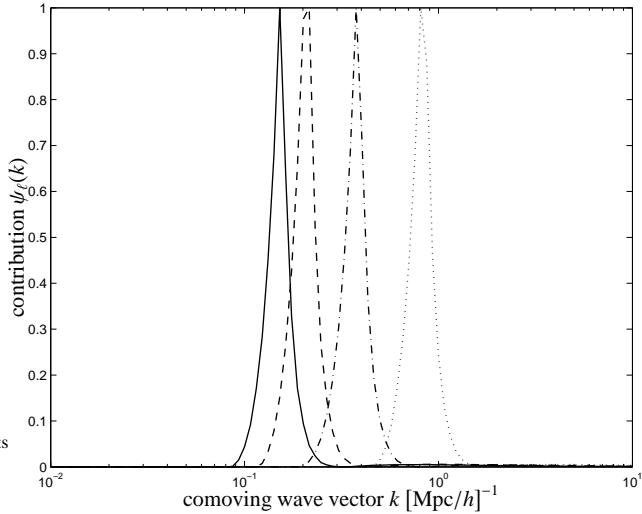


Figure 6. Contribution $\psi_\ell(k)$ of the 4-point term to the angular power spectrum $C_\tau(\ell)$ of the iSW temperature fluctuations τ as a function of wave vector k , for $\ell = 100$ (solid line), $\ell = 300$ (dashed line), $\ell = 1000$ (dash-dotted line) and $\ell = 3000$ (dotted line). The curves have been normalised to a peak value of unity.

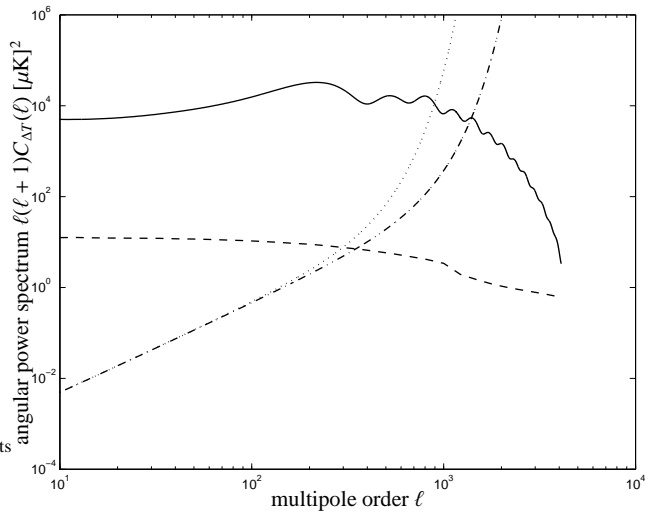


Figure 7. Angular power spectrum $C_{\Delta T}(\ell) = T_{\text{CMB}}^2 C_\tau(\ell)$ of the iSW temperature fluctuations $\tau(\theta)$ (dashed line). The CMB power spectrum $C_{\text{CMB}}(\ell)$ for the ΛCDM model (solid line) and the limiting *Planck*-sensitivities $C_{\text{noise}}(\ell)$ for angular resolutions $\Delta\theta = 5'0$ (dash-dotted line) and $\Delta\theta = 9'1$ (dotted line) are depicted for comparison.

$$\frac{1}{\sigma_{\text{eff}}^2} = \sum_{i=1}^6 \frac{1}{\sigma_i^2} \rightarrow \sigma_{\text{eff}} = 13.42 \mu\text{K}. \quad (76)$$

The sensitivity considerations suggest that the iSW-effect is well above the noise level of the combined *Planck* HFI-channels, so that the power spectrum of $C_\tau(\ell)$ should be observable for angular scales $\ell \lesssim 200$ as a contribution to the primary CMB fluctuations $C_{\text{CMB}}(\ell)$, which in Fig. 7 have been computed using the CMBfast code by Seljak & Zaldarriaga (1996). The signal can of course be amplified by cross-correlation with a suitable population of tracer galaxies.

5 SUMMARY

The scope of this paper is to derive the corrections to the power spectrum of weak gravitational lensing due to gravitomagnetic terms in the metric by perturbation theory. Within the same formalism, the power spectrum of the iSW-effect can be determined as well.

- The iSW-effect and gravitomagnetic lensing measure the evolution of velocities and densities in the large-scale structure and are sensitive to the cosmological parameters Ω_M and σ_8 . Applied to single objects like clusters, where the above described formalism equally applies, the iSW-effect would allow to measure the cosmological evolution of merger rates and dark matter accretion strengths (van den Bosch 2002; Wechsler et al. 2002; Zhao et al. 2003).

- Gravitomagnetic lensing would test general relativity on the largest scales (Mpc - Gpc) to second order in v/c , and could help to decide in favour of or against other metric theories of gravity. It should be emphasised that in the current theoretical description of structure formation or in current numerical simulations the motion of bodies is described by classical mechanics, i.e. instantaneous propagation of potentials and no relativistic increase of inertial mass with velocity, but the interaction of light with matter should be treated in the framework of the post-Newtonian limits of general relativity.

- Gravitomagnetic terms influence the weak lensing power spectrum most notably on large spatial and angular scales, which are difficult to access experimentally. Furthermore, cosmic variance and galactic foregrounds prevent accurate measurements on the scales in question, i.e. $\gtrsim \text{Gpc}/h$ and above. The small gravitomagnetic corrections could be amplified by cross correlation with the kinetic Sunyaev-Zel'dovich effect (Sunyaev & Zel'dovich 1972), once future CMB telescopes will provide accurate measurements of line-of-sight velocities or with the velocity information from optical galaxy surveys. For contemporary weak lensing surveys, gravitomagnetic corrections to the cosmic shear do not play a significant role.

- The iSW-effect is described by a line-of-sight integration over the divergence of the gravitomagnetic potentials. By this argument, the iSW-effect is reduced to a second order lensing effect. Every iSW quantity has a correspondence in weak gravitational lensing and the derivation of the power spectrum $C_\tau(\ell)$ proceeds in complete analogy to that of any weak lensing quantity, for instance that of the convergence $C_\kappa(\ell)$. The most important difference of the derivation presented here to the ones carried out by Seljak (1996) or Cooray (2002) is that our derivation explicitly pays tribute to the lensing nature of the iSW-effect.

- Gravitomagnetic lensing and the iSW-effect are complementary in measuring the matter flows parallel and perpendicular to the line-of-sight. The picture emerging is that (subject to the approximations made) in gravitational light deflection (including the gravitomagnetic term A_z), the photon's \mathbf{k} -vector is rotated but its normalisation is conserved. Contrarily, the components of \mathbf{A} transverse to the line-of-sight change the normalisation of the \mathbf{k} -vector, i.e. the photon's energy, but leave the direction of \mathbf{k} invariant.

- Both effects, gravitomagnetic lensing and the iSW-effect, are achromatic which makes them only accessible by their n -point statistics. Furthermore, the iSW-effect needs to be separated from other achromatic CMB structures such as the kinetic Sunyaev-Zel'dovich effect and the Ostriker-Vishniac effect. The derivation predicts iSW temperature fluctuations of a few μK on large angular scales, which is within reach of future CMB experiments like the

European *Planck*-mission^{3,4}, provided that the modelling of Galactic foregrounds is sufficiently accurate to access these large angular scales.

- The gradient $\chi(\theta)$ of the iSW temperature fluctuation field $\tau(\theta)$ should directly map regions of large matter flows, e.g. filaments and clusters with high peculiar velocities, but it can be expected to be very susceptible to noise due to the differentiation required in obtaining $\chi(\theta)$ from $\tau(\theta)$, which is reflected by the fact that ratio of the angular power spectra $C_\chi(\ell)/C_\tau(\ell)$ is proportional to $\ell(\ell+1)$.

The verification of the theoretical approach by a ray-tracing simulation of photons through a cosmological n -body simulation will be the subject of a future paper. The non-Gaussian features the iSW-effect and gravitational lensing exhibit and the mode-coupling in nonlinear structure growth are unaccessible to perturbation theory and are important on small scales. The novel approach to the iSW-effect presented here should allow a much improved precision in the numerical treatment, because inaccuracies in interpolating the scalar potential's time derivative $\partial\Phi/\partial t$ for each integration time step and in integrating a rapidly oscillating function inherent the direct approach (e.g. Tuluie & Laguna 1995a,b) are alleviated.

ACKNOWLEDGEMENTS

We would like to thank T. A. Enßlin for reading the manuscript. For numerical evaluation of the Bessel functions $J_\ell(x)$ and their derivatives $dJ_\ell(x)/dx$ an excerpt taken from the CMBfast code⁵ written by Seljak & Zaldarriaga (1996) was used.

APPENDIX A: DECOMPOSITION OF MIXED 3-POINT CORRELATORS OF DENSITY AND VELOCITY FIELDS

In order to evaluate the 3-point correlation function $\langle\delta(\mathbf{k}_1)v(\mathbf{k}_2)\delta(\mathbf{k}_3)\rangle$ in perturbation theory, the density- and velocity fields are decomposed into linear terms $\delta^{(1)}, v^{(1)}$ and small perturbations $\delta^{(2)}, v^{(2)}$:

$$\delta(\mathbf{k}) = \delta^{(1)}(\mathbf{k}) + \delta^{(2)}(\mathbf{k}) \text{ and } v(\mathbf{k}) = v^{(1)}(\mathbf{k}) + v^{(2)}(\mathbf{k}). \quad (\text{A1})$$

As shown by Fry (1984), the second order density perturbation can be written as:

$$\begin{aligned} \delta^{(2)}(\mathbf{k}) &= \int \frac{d^3p}{(2\pi)^3} \int \frac{d^3p'}{(2\pi)^3} (2\pi)^3 \delta_D(\mathbf{p} + \mathbf{p}' - \mathbf{k}) M(\mathbf{p}, \mathbf{q}) \delta(\mathbf{p}) \delta(\mathbf{p}') \\ &= \int \frac{d^3p}{(2\pi)^3} M(\mathbf{p}, \mathbf{k} - \mathbf{p}) \delta^{(1)}(\mathbf{p}) \delta^{(1)}(\mathbf{k} - \mathbf{p}), \end{aligned} \quad (\text{A2})$$

with the function $M(\mathbf{p}, \mathbf{p}')$ being defined as:

$$M(\mathbf{p}, \mathbf{p}') = \frac{10}{7} + \frac{\mathbf{p}\mathbf{p}'}{pp'} \left(\frac{p}{p'} + \frac{p'}{p} \right) + \frac{4}{7} \left(\frac{\mathbf{p}\mathbf{p}'}{pp'} \right)^2. \quad (\text{A3})$$

Clearly, the function M is symmetric, $M(\mathbf{p}, \mathbf{p}') = M(\mathbf{p}', \mathbf{p})$ and has the properties that $M(-\mathbf{p}, -\mathbf{p}') = M(\mathbf{p}, \mathbf{p}')$ and $M(-\mathbf{p}, \mathbf{p}') = M(\mathbf{p}, -\mathbf{p}')$. For the first order perturbation of the velocity field, one obtains:

$$v^{(2)}(\mathbf{k}) = -iH(a)f(\Omega) \frac{\mathbf{k}}{k^2} \delta^{(2)}(\mathbf{k}). \quad (\text{A4})$$

The 3-point correlation function $\langle\delta(\mathbf{k}_1)v(\mathbf{k}_2)\delta(\mathbf{k}_3)\rangle$ can now be expanded to yield to second order:

$$\langle\delta(\mathbf{k}_1)v(\mathbf{k}_2)\delta(\mathbf{k}_3)\rangle \simeq \langle\delta^{(1)}(\mathbf{k}_1)v^{(1)}(\mathbf{k}_2)\delta^{(2)}(\mathbf{k}_3)\rangle + (\text{cycl}) + O(2) \quad (\text{A5})$$

with the zeroth order term $\langle\delta^{(1)}(\mathbf{k}_1)v^{(1)}(\mathbf{k}_1)\delta^{(1)}(\mathbf{k}_1)\rangle$ vanishing due to $v^{(1)}(\mathbf{k}) \propto \delta^{(1)}(\mathbf{k})$ for truly Gaussian random fields. If the perturbation is contained in the density field δ , inserting eqn. (A2) into the correlator yields:

$$\begin{aligned} \langle\delta^{(1)}(\mathbf{k}_1)v^{(1)}(\mathbf{k}_2)\delta^{(2)}(\mathbf{k}_3)\rangle &= \int \frac{d^3p}{(2\pi)^3} \int \frac{d^3p'}{(2\pi)^3} \times \\ &(2\pi)^3 \delta_D(\mathbf{p} + \mathbf{p}' - \mathbf{k}_3) M(\mathbf{p}, \mathbf{p}') \langle\delta(\mathbf{k}_1)\delta(\mathbf{p})\rangle \langle\delta(\mathbf{p}')v(\mathbf{k}_2)\rangle. \end{aligned} \quad (\text{A6})$$

Similarly, if the perturbation is the velocity-field v , one obtains:

$$\begin{aligned} \langle\delta^{(1)}(\mathbf{k}_1)v^{(2)}(\mathbf{k}_2)\delta^{(1)}(\mathbf{k}_3)\rangle &= \int \frac{d^3p}{(2\pi)^3} \int \frac{d^3p'}{(2\pi)^3} \times \\ &(2\pi)^3 \delta_D(\mathbf{p} + \mathbf{p}' - \mathbf{k}_2) M(\mathbf{p}, \mathbf{p}') \langle\delta(\mathbf{k}_1)v(\mathbf{p})\rangle \langle v(\mathbf{p}')\delta(\mathbf{k}_3)\rangle. \end{aligned} \quad (\text{A7})$$

Collecting these results for the mixed 3-point correlator of density and velocity fields in question yields for the first order expansion of $\langle\delta(\mathbf{k}_1)v(\mathbf{k}_2)\delta(\mathbf{k}_3)\rangle$ in perturbation theory:

$$\langle\delta^{(1)}(\mathbf{k}_1)v^{(1)}(\mathbf{k}_2)\delta^{(2)}(\mathbf{k}_3)\rangle = M(\mathbf{k}_1, \mathbf{k}_2) P_{\delta\delta}(|\mathbf{k}_1|) P_{\delta v}(|\mathbf{k}_2|), \quad (\text{A8})$$

$$\langle\delta^{(1)}(\mathbf{k}_1)v^{(2)}(\mathbf{k}_2)\delta^{(1)}(\mathbf{k}_3)\rangle = M(\mathbf{k}_1, \mathbf{k}_3) P_{\delta v}(|\mathbf{k}_1|) P_{\delta v}(|\mathbf{k}_3|), \quad (\text{A9})$$

$$\langle\delta^{(2)}(\mathbf{k}_1)v^{(1)}(\mathbf{k}_2)\delta^{(1)}(\mathbf{k}_3)\rangle = M(\mathbf{k}_2, \mathbf{k}_3) P_{\delta\delta}(|\mathbf{k}_2|) P_{\delta v}(|\mathbf{k}_3|), \quad (\text{A10})$$

if the condition $\sum_{i=1}^3 \mathbf{k}_i = \mathbf{0}$ is fulfilled. Hence, in first order perturbation theory, the 3-point correlation function can be decomposed into products of the density-density and density-velocity correlation functions, which are of the order v/c (eqns. A8 and A10), and into the square of the density-velocity cross correlation, which is of order v^2/c^2 (eqn. A9).

REFERENCES

- Abramowitz M., Stegun I. A., 1972, Handbook of Mathematical Functions. Handbook of Mathematical Functions, New York: Dover, 1972
- Afshordi N., Loh Y., Strauss M. A., 2004, Phys. Rev. D, 69, 083524
- Bardeen J. M., Bond J. R., Kaiser N., Szalay A. S., 1986, ApJ, 304, 15
- Bartelmann M., Schneider P., 2001, Physics Reports, 340, 291
- Bernardeau F., 1997, A&A, 324, 15
- Blandford R. D., Saust A. B., Brainerd T. G., Villumsen J. V., 1991, MNRAS, 251, 600
- Boughn S., Crittenden R., 2004, Nature, 427, 45
- Carroll S. M., Press W. H., Turner E. L., 1992, ARA&A, 30, 499
- Colberg J. M., Krughoff K. S., Connolly A. J., 2004, ArXiv Astrophysics e-prints
- Colberg J. M., White S. D. M., MacFarland T. J., Jenkins A., Pearce F. R., Frenk C. S., Thomas P. A., Couchman H. M. P., 2000, MNRAS, 313, 229
- Cooray A., 2002, Phys. Rev. D, 65, 083518
- Crittenden R. G., Turok N., 1996, Physical Review Letters, 76, 575
- Dekel A., 1994, ARA&A, 32, 371
- Efstathiou G., Bond J. R., White S. D. M., 1992, MNRAS, 258, 1P

³ <http://planck.mpa-garching.mpg.de/>

⁴ <http://astro.estec.esa.nl/Planck/>

⁵ <http://www.cmbfast.org>

- Ellis R. S., 1997, *ARA&A*, 35, 389
- Fomalont E. B., Kopeikin S. M., 2003, *ApJ*, 598, 704
- Fosalba P., Gaztañaga E., Castander F. J., 2003, *ApJL*, 597, L89
- Fry J. N., 1984, *ApJL*, 277, L5
- Heyrovsky D., 2004, *ArXiv Astrophysics e-prints*
- Hirata C. M., Padmanabhan N., Seljak U., Schlegel D., Brinkmann J., 2004, *ArXiv Astrophysics e-prints*
- Hu W., Sugiyama N., 1994, *Phys. Rev. D*, 50, 627
- Ibanez J., 1983, *A&A*, 124, 175
- Jaffe A. H., Kamionkowski M., 1998, *Phys. Rev. D*, 58, 043001
- Jain B., Seljak U., 1997, *ApJ*, 484, 560
- Jenkins A., Frenk C. S., White S. D. M., Colberg J. M., Cole S., Evrard A. E., Couchman H. M. P., Yoshida N., 2001, *MNRAS*, 321, 372
- Kaiser N., 1982, *MNRAS*, 198, 1033
- Kaiser N., Squires G., 1993, *ApJ*, 404, 441
- Knox L., 1995, *Phys. Rev. D*, 52, 4307
- Lahav O., Rees M. J., Lilje P. B., Primack J. R., 1991, *MNRAS*, 251, 128
- Ménard B., Erben T., Mellier Y., 2003, in *Matter and Energy in Clusters of Galaxies*, ASP Conference Proceedings, Vol. 301. Held 23-27 April 2002 at National Central University, Chung-Li, Taiwan. Edited by Stuart Bowyer and Chorng-Yuan Hwang. San Francisco: Astronomical Society of the Pacific, 2003. ISBN: 1-58381-149-4, p.537 Weak Lensing Study of Abell 2029. p. 537
- Ma C., Fry J. N., 2002, *Physical Review Letters*, 88, 211301
- Martínez-González E., Sanz J. L., 1990, *MNRAS*, 247, 473
- Martínez-González E., Sanz J. L., Silk J., 1990, *ApJL*, 355, L5
- Martínez-González E., Sanz J. L., Silk J., 1992, *Phys. Rev. D*, 46, 4193
- Martínez-González E., Sanz J. L., Silk J., 1994, *ApJ*, 436, 1
- Monin A. S., Yaglom A. M., 1965a, *Statistical Fluid Mechanics: Mechanics of Turbulence (Volume 1)*. The MIT Press
- Monin A. S., Yaglom A. M., 1965b, *Statistical Fluid Mechanics: Mechanics of Turbulence (Volume 2)*. The MIT Press
- Nolta M. R., Wright E. L., Page L., Bennett C. L., Halpern M., Hinshaw G., Jarosik N., Kogut A., Limon M., Meyer S. S., Spergel D. N., Tucker G. S., Wollack E., 2004, *ApJ*, 608, 10
- Ostriker J. P., Vishniac E. T., 1986, *ApJL*, 306, L51
- Peebles P. J. E., 1980, *The large-scale structure of the universe*. Research supported by the National Science Foundation. Princeton, N.J., Princeton University Press, 1980. 435 p.
- Rees M. J., Sciama D. W., 1968, *Nature*, 217, 511
- Rubiño-Martín J. A., Hernández-Monteagudo C., Enßlin T. A., 2004, *A&A*, 419, 439
- Sachs R. K., Wolfe A. M., 1967, *ApJ*, 147, 73
- Schneider P., Ehlers J., Falco E. E., 1992, *Gravitational Lenses*. Springer-Verlag Berlin Heidelberg New York.
- Schneider P., van Waerbeke L., Jain B., Kruse G., 1998, *MNRAS*, 296, 873
- Seitz C., Kneib J.-P., Schneider P., Seitz S., 1996, *A&A*, 314, 707
- Seljak U., 1996, *ApJ*, 460, 549
- Seljak U., Zaldarriaga M., 1996, *ApJ*, 469, 437
- Sereno M., 2003, *MNRAS*, 344, 942
- Spergel D. N., Verde L., Peiris H. V., Komatsu E., Nolta M. R., Bennett C. L., Halpern M., Hinshaw G., Jarosik N., Kogut A., Limon M., Meyer S. S., Page L., Tucker G. S., Weiland J. L., Wollack E., Wright E. L., 2003, *ApJ*, submitted, astro-ph/0302209
- Strauss M. A., Willick J. A., 1995, *Physics Reports*, 261, 271
- Sugiyama N., 1995, *ApJS*, 100, 281
- Sunyaev R. A., Zel'dovich I. B., 1972, *Comments Astrophys. Space Phys.*, 4, 173
- Takada M., Jain B., 2003a, *MNRAS*, 340, 580
- Takada M., Jain B., 2003b, *MNRAS*, 344, 857
- Tegmark M., Efstathiou G., 1996, *MNRAS*, 281, 1297
- Tuluie R., Laguna P., 1995a, in *Seventeenth Texas Symposium on Relativistic Astrophysics and Cosmology Chasing CMB Photons through the Nonlinear Universe..* p. 692
- Tuluie R., Laguna P., 1995b, *ApJL*, 445, L73
- van den Bosch F. C., 2002, *MNRAS*, 331, 98
- van Waerbeke L., Mellier Y., Erben T., Cuillandre J. C., Bernardeau F., Maoli R., Bertin E., Mc Cracken H. J., Le Fèvre O., Fort B., Dantel-Fort M., Jain B., Schneider P., 2000, *A&A*, 358, 30
- Vishniac E. T., 1987, *ApJ*, 322, 597
- Watson G. N., 1952, *A treatise on the theory of Bessel functions*. Cambridge University Press, Cambridge, 1952
- Wechsler R. H., Bullock J. S., Primack J. R., Kravtsov A. V., Dekel A., 2002, *ApJ*, 568, 52
- Zhao D. H., Mo H. J., Jing Y. P., Börner G., 2003, *MNRAS*, 339, 12

This paper has been typeset from a $\text{\TeX}/\text{\LaTeX}$ file prepared by the author.